

# UCSF

## UC San Francisco Previously Published Works

### Title

Spatiotemporal characteristics of neurophysiological changes in patients with four-repeat tauopathies

### Permalink

<https://escholarship.org/uc/item/7206c3t7>

### Journal

Annals of Clinical and Translational Neurology, 11(2)

### ISSN

2328-9503

### Authors

Samudra, Niyatee

Lerner, Hannah

Yack, Leslie

et al.

### Publication Date

2024-02-01


### DOI

10.1002/acn3.51974

Peer reviewed

## CASE STUDY

# Spatiotemporal characteristics of neurophysiological changes in patients with four-repeat tauopathies

Niyatee Samudra<sup>1,†</sup>, Hannah Lerner<sup>1,†</sup>, Leslie Yack<sup>1,2</sup>, Christine M. Walsh<sup>1</sup>, Heidi E. Kirsch<sup>3,4</sup>, Kiwamu Kudo<sup>3,5</sup>, Claire Yballa<sup>1</sup>, Renaud La Joie<sup>1</sup>, Maria L. Gorno-Tempini<sup>1</sup>, Salvatore Spina<sup>1</sup>, William W. Seeley<sup>1</sup>, Thomas C. Neylan<sup>1,2</sup>, Bruce L. Miller<sup>1</sup>, Gil D. Rabinovici<sup>1,3</sup>, Adam Boxer<sup>1</sup>, Lea T. Grinberg<sup>1,6,7</sup>, Katherine P. Rankin<sup>1</sup>, Srikantan S. Nagarajan<sup>3</sup> & Kamalini G. Ranasinghe<sup>1</sup> 

<sup>1</sup>Memory and Aging Center, Department of Neurology, Weill Institute for Neurosciences, University of California San Francisco, San Francisco, California, 94158, USA

<sup>2</sup>Department of Psychiatry, San Francisco Veterans Affairs, University of California San Francisco, San Francisco, California, 94158, USA

<sup>3</sup>Department of Radiology and Biomedical Imaging, University of California San Francisco, San Francisco, California, 94143, USA

<sup>4</sup>Epilepsy Center, Department of Neurology, University of California San Francisco, San Francisco, California, USA

<sup>5</sup>Medical Imaging Business Center, Ricoh Company, Kanazawa, Japan

<sup>6</sup>Department of Pathology, University of California, San Francisco, California, 94158, USA

<sup>7</sup>Department of Pathology, University of Sao Paulo Medical School, Sao Paulo, Brazil

## Correspondence

Kamalini G. Ranasinghe, Memory and Aging Center, Department of Neurology, University of California San Francisco, 675 Nelson Rising Lane, Suite 190, San Francisco, CA 94158-1207, USA. Tel: 415-514-8847; E-mail: [kamalini.ranasinghe@ucsf.edu](mailto:kamalini.ranasinghe@ucsf.edu)

## Funding Information

This study was supported by the National Institutes of Health grants: K08AG058749 (KGR), 1R21AG077498-01 (KGR), P30 AG062422, P01 AG19724 (BLM), P50-AG023501 (BLM & GDR), R01 AG045611 (GDR); K99AG065501 (RLJ); NS100440 (SSN), DC176960 (SSN), DC017091 (SSN), AG062196 (SSN); R01AG060477 (LTG), R01 AG064314 (LTG), K24 AG053435 (LTG), R01 AG075802 (LTG), R01 AG AG070826 (LTG); grants from Larry L. Hillblom Foundation: 2015-A-034-FEL and (KGR); 2019-A-013-SUP (KGR); a grant from the Alzheimer's Association: AARG-21-849773 (KGR).

Received: 18 August 2023; Revised: 1 December 2023; Accepted: 5 December 2023

*Annals of Clinical and Translational Neurology* 2024; 11(2): 525–535

doi: 10.1002/acn3.51974

<sup>†</sup>These authors contributed equally.

## Abstract

**Introduction:** Progressive supranuclear palsy (PSP) and corticobasal degeneration (CBD), are the most common four-repeat tauopathies (4RT), and both frequently occur with varying degree of Alzheimer's disease (AD) copathology. Intriguingly, patients with 4RT and patients with AD are at opposite ends of the wakefulness spectrum—AD showing reduced wakefulness and excessive sleepiness whereas 4RT showing decreased homeostatic sleep. The neural mechanisms underlying these distinct phenotypes in the comorbid condition of 4RT and AD are unknown. The objective of the current study was to define the alpha oscillatory spectrum, which is prominent in the awake resting-state in the human brain, in patients with primary 4RT, and how it is modified in comorbid AD-pathology. **Method:** In an autopsy-confirmed case series of 4R-tauopathy patients ( $n = 10$ ), whose primary neuropathological diagnosis was either PSP ( $n = 7$ ) or CBD ( $n = 3$ ), using high spatiotemporal resolution magnetoencephalography (MEG), we quantified the spectral power density within alpha-band (8–12 Hz) and examined how this pattern was modified in increasing AD-copathology. For each patient, their regional alpha power was compared to an age-matched normative control cohort ( $n = 35$ ). **Result:** Patients with 4RT showed increased alpha power but in the presence of AD-copathology alpha power was reduced. **Conclusions:** Alpha power increase in PSP-tauopathy and reduction in the presence of AD-tauopathy is consistent with the observation that neurons activating wakefulness-promoting systems are preserved in PSP but degenerated in AD. These results highlight the selectively vulnerable impacts in 4RT versus AD-tauopathy that may have translational significance on disease-modifying therapies for specific proteinopathies.

## Introduction

Four-repeat tauopathies (4RT) are neurodegenerative disorders associated with abnormal cytoplasmic inclusions of tau protein isoforms with four microtubule-binding domains.<sup>1</sup> The two most common clinical presentations of 4RT include the Richardson syndrome variant of progressive supranuclear palsy (PSP-Richardson) and the corticobasal syndrome (CBS). Alzheimer's disease (AD), which is a tauopathy of three- and four-repeat tau, is a common copathology in both disorders. Intriguingly, 4R tauopathies and AD are on opposite ends of the wake-sleep cycle. Patients with 4RT, particularly PSP, exhibit decreased homeostatic sleep,<sup>2–4</sup> whereas patients with AD have reduced wakefulness with excessive daytime sleepiness and sundowning.<sup>5</sup> Consistent with these clinical phenotypes, neuropathological studies have shown that wakefulness-promoting subcortical neurons are selectively vulnerable in AD but spared in PSP.<sup>5,6</sup> The functional consequences of comorbid AD and 4RT on neural circuits in wakefulness remain largely unknown. Although it may be clinically silent, comorbid AD may still be consequential to neurophysiological disease manifestations, hence an important consideration for disease-modifying clinical trials targeting 4R tauopathies.<sup>7</sup>

Neural oscillations represent the electrical activity of synchronous firing of organized neural circuits. The most characteristic oscillatory activity in the awake human brain is alpha rhythm that oscillates between 8 and 12 Hz. Greater spectral power within alpha oscillatory band in electrophysiological recordings is reliably associated with relaxed wakefulness in the human brain<sup>8</sup> while change of brain states from awake to sleep-onset is characterized by a reduction in alpha activity. Consistent with such phenomenon, patients with AD who clinically have impaired wakefulness show a dramatic reduction of alpha the power in oscillatory spectrum. Prior work from our group have shown that this reduced alpha oscillatory activity in AD patients is correlated with regional accumulation of tau.<sup>9,10</sup> Neuropathological studies have further shown that wakefulness-promoting neurons are among the earliest targets of AD-tauopathy. While the loss of wakefulness-promoting neurons and altered wakefulness forms a consistent representation with reduced alpha power in AD-tauopathy, much less is known about these relationships in primary 4RT syndromes as well as the frequent condition of their co-occurrence. Because AD and 4RT diverge in their wakefulness phenotype, it remains to be shown what happens to alpha oscillatory patterns in the condition of 4RT and AD-copathology.

Here, we evaluated 10 patients with clinically suspected 4R tauopathy antemortem, who were demonstrated to

have either PSP or CBD as their primary neuropathology at autopsy. Using high spatiotemporal resolution of magnetoencephalography (MEG) imaging to characterize the finer details of abnormal oscillatory spectral signatures we relate these to specific neuropathological findings of primary 4R tauopathy and associated AD-copathology. We hypothesized that, consistent with the divergent wakefulness phenotypes of 4RT and AD—alpha power will decrease with AD comorbidity.

## Methods

Here, we present a case series of 10 patients, with clinically suspected 4RT antemortem, and a primary neuropathology of PSP or CBD at autopsy, evaluated at the University of California San Francisco, Memory and Aging Center (Table 1). Clinical diagnoses were established after a multidisciplinary consensus meeting. Informed consent was obtained from all participants. The study was approved by the UCSF Institutional Review Board (IRB). All participants underwent 10–45-min resting state MEG recording, and postmortem neuropathological assessment. Three participants were further evaluated with polysomnography (PSG; Table S1) and six with positron emission tomography (PET) with amyloid binding tracers (Table 2). The full details of each patients' clinical presentation are presented in the supplement.

## Neuropathology

At autopsy, brain tissue was obtained postmortem, processed, and analyzed according to standard protocols, as previously described.<sup>11</sup> Primary pathological diagnosis was herein defined as the most developed neuropathological entity in which severity and regional distribution were thought to explain the majority of the patient's clinical cognitive and behavioral phenotype.<sup>12</sup> The pathologic diagnoses of PSP, CBD, as well as Lewy body disease, were completed based on previously published consensus guidelines.<sup>13–16</sup> The presence of additional AD pathology was also defined. AD pathologic assessment followed NIA-AA guidelines.<sup>17</sup> All cases were classified according to the Alzheimer's disease neuropathological change (ADNC) severity (i.e., ABC score), including Thal phase, Braak Stage, and Consortium to Establish a Registry for Alzheimer's Disease (CERAD) neuritic plaque frequency stage.<sup>12</sup> AD neuropathologic change severity is a synthesis of these features into a single descriptor: no AD, low, intermediate, or high degree of AD neuropathologic change.

**Table 1.** Clinical history and neurological exam findings.

Patient	Age (sex)	Clinical syndromic diagnosis	Clinical history features	Neuro exam findings	Disease duration-years	MEG to death-years
P1	80–90 (F)	PSP	Multiple falls, blepharospasm, cognitive decline, some response to carbidopa-levodopa.	Vertical > horizontal apraxia of extraocular eye movements, axial rigidity, retropulsion, gait apraxia, RUL dystonic posture, R & LUL bradykinesia.	14	2
P2	70–80 (M)	PSP-Richardson	Pill-rolling tremor, handwriting changes, balance difficulties and falls, word finding difficulties, perseverative, and compulsive behaviors (sexual).	Postural instability, supranuclear gaze palsy, axial rigidity, RUL apraxia and dystonia, disinhibition, stimulus-bound behaviors.	9	3
P3	70–80 (F)	nfvPPA with CBS	Slowing of speech, word substitutions, effortful speech, gait instability, dysphagia, difficulty using right hand.	Speech apraxia, dystonic posturing of right hand, decreased right arm swing.	7	2
P4	80–90 (M)	nfvPPA with PSP	Progressive decline in language output, slurred speech.	Apraxic speech, decreased amplitude and slowed initiation of horizontal and vertical saccades, LUL bradykinesia, decreased right arm swing, difficulty with tandem gait.	7	3
P5	80–90 (M)	nfvPPA with CBS	Apathy, decreased motivation, social withdrawal, compulsions, phonemic and grammatical errors, decreased speech output, slurred speech, mild tremors, gait difficulties.	Decreased saccadic initiation and velocity (upgaze > downgaze), wide-based gait, decreased right arm swing, mild retropulsion.	9	4
P6	70–80 (F)	PSP-Richardson	Micrographia, imbalance and falls, difficulty with multitasking, impulsivity, emotional frustration, pseudobulbar affect, hypophonia, dysphagia.	Hypomimia, square-wave jerks, hypometric saccades, decreased blink rate, RUL hypertonia, right hemibody decreased temperature sensation, gait instability with spontaneous retropulsion.	13	3
P7	70–80 (M)	PSP-Richardson	Dysexecutive and amnesic symptoms, voice changes, double vision, dysphagia, increasing falls, depression.	Decreased ocular pursuit, increased latency and reduced speed in vertical saccades, axial and UL rigidity, Parkinsonian gait, R > L resting and postural tremors.	9	3
P8	60–70 (M)	CBS	Speech and motor difficulty (decreased dexterity; dystonic posture of the right hand), depression, poor sleep, excessive interest in sweets, dysexecutive symptoms.	Effortful and dysarthric speech with frequent pauses, decreased amplitude, initiation and velocity in both vertical and horizontal saccades, LUL ideomotor apraxia astereognosis, agraphesthesia, right arm dystonia, shuffling gait, bilateral decreased arm swing.	5	3
P9	70–80 (F)	nfvPPA	Speech difficulties (effortful production, mispronunciations, diminished output), executive dysfunction, gait imbalance.	Speech and orobuccal apraxia, spastic dysarthria, axial rigidity, LUL tremor, and decreased arm swing.	8	6
P10	60–70 (M)	PSP	Repeated falls, paucity of speech, irritability, repetitive behaviors, hypersexuality, hyperorality, parkinsonism, dysphagia.	Vertical > horizontal decreased saccadic amplitude, initiation and velocity, hypomimia, hypophonia, R&LUL hypertonia, L > R bradykinesia, decreased right arm swing	4	0

CBS, corticobasal syndrome; MEG, magnetoencephalography; L, left; LUL, left upper limb; nfvPPA, non fluent variant of primary progressive aphasia; PSP, progressive supranuclear palsy; R, right; R & L, right and left; RUL, right upper limb.

**Table 2.** Neuropathological findings.

Patient	Primary neuropathology	AD neuropathological change (ADNC) (NIA-AA)	Braak (NFT)	Comorbid pathological diagnoses	Amyloid PET visual read (centiloid)
P1	PSP	No (A0, B1, C0)	2	AGD, ART, CAA, TDP43, ARTAG	<i>na</i>
P2	PSP	Low (A1, B1, C0)	2	ADNC, AGD, Art, CAA, ARTAG	Negative (18)
P3	PSP	Low (A1, B1, C0)	2	ADNC, Vas, Art, ARTAG	Negative (6)
P4	PSP	Low (A1, B1, C0)	2	ADNC, LBD, Art	<i>na</i>
P5	PSP	Low (A1, B2, C0)	4	ADNC, AGD, Art, ARTAG	Negative (3)
P6	PSP	Low (A1, B2, C0)	4	ADNC, CAA, AGD, Art, Vas	<i>na</i>
P7	PSP	Intermediate (A3, B2, C2)	3	AD, CAA, AGD, ARTAG, Art	Positive (69)
P8	CBD	Low (A1, B1, C1)	2	ADNC, AGD, Art	Negative (3)
P9	CBD	Low (A1, B1, C2)	2	ADNC	Negative (1)
P10	CBD	Low (A2, B1, C2)	1	ADNC, Art	<i>na</i>

Centiloid values above 24.4 are consistent with intermediate-to-high ADNC. ADNC, Alzheimer's disease neuropathological change; AGD, argyrophilic grain disease; Art, arteriolosclerosis; ARTAG, aging-related tau astroglipathy; CAA, cerebral amyloid angiopathy; LBD, Lewy body disease; TDP43, TAR DNA-binding protein 43; Vas, vascular brain injury; (*na*), not available.

### Magnetoencephalography (MEG) and electroencephalography (EEG)

Resting-state MEG was performed at the UCSF Biomagnetic Imaging Laboratory with a whole-head MEG system (CTF, Port Coquitlam, British Columbia, Canada) comprising 275 axial gradiometers (sampling rate = 600 Hz). P3, P4, P5, P8, and P9 had MEG only (10–30 min), while the others had MEG with simultaneous EEG for 60 min. EEG was recorded using the standard 10–20 system with 19 electrodes. MEG and EEG were reviewed for gross asymmetry and epileptiform discharges by two epileptologists (NS and HK) and a neurophysiologist (KGR). Fiducial coils were placed at the nasion and left and right preauricular points to locate head position relative to the sensor array, and later used to co-register with the brain MRI. Data collection was optimized to minimize within-session head movements and to keep it below 0.5 cm.

Sixty seconds of continuous MEG recording was selected from each subject while lying supine and awake with eyes closed, with minimal artifacts (i.e., minimal excessive scatter at signal amplitude) for quantitative analyses. The MEG, and concomitant EEG where available, were visualized to confirm the resting, awake, state of each patient during the 60-s epochs.<sup>10</sup> Subjects were instructed to keep eyes closed during the data collection. Additional data inspection and screening was also employed by visualizing the 1–70 Hz oscillatory activity in the MEG and EEG (where available) using the clinical CTF-M/EEG DataEditor software to confirm that the continuous 60-s data epoch selected for analysis does not include eyeblink artifacts. The preprocessing and source reconstructions were performed using in-house Matlab scripts utilizing Fieldtrip toolbox.<sup>18</sup> Isotropic voxels (5 mm) were generated in a brain region of a template

MRI. The generated voxels were warped into individualized head-shape and then magnetic lead-field vectors were computed on each voxel using a single-shell model approximation.<sup>19</sup> The voxels for each subject were indexed to the 246 cortical regions defined in the brainnetome atlas.<sup>20</sup> We used BrainNet Viewer toolbox to obtain brain rendering images of MEG metrics.<sup>21</sup> Based on the 246 regional time-course data, we computed the relative spectral power within two canonical frequency bands 2–7 Hz (delta-theta), and 8–12 Hz (alpha). The spectral power (relative spectral power) of a given band was defined by the ratio of a band power to the total power. Regional spectral power was computed from the 246 regional time-course data using the Welch's method (50% overlapping) with a 0.293 Hz (= fs/2048) step.

### Polysomnography (PSG)

Nocturnal PSG and videos were digitally recorded for three patients (P2, P6, and P7) at 400 Hz using a portable sleep monitoring system (Beehive@Horizon, Grass Technologies, West Warwick, RI, USA).<sup>3</sup> Recording parameters were as noted in previous literature.<sup>3</sup> The overnight PSG was used to identify measures of interest, such as latency to sleep onset, wake time after sleep onset, total sleep time, sleep efficiency, and percent time in N1 sleep, N2 sleep, N3 sleep, and REM sleep. Latency to REM sleep as well as apnea/hypopnea index (AHI) and periodic limb movement index (PLMI) were also studied.

### Positron emission tomography (PET)

Amyloid PET (<sup>11</sup>C-PIB) was completed for cases P2, P3, P5, P7, P8, and P9. Tau PET (flortaucipir) was completed for cases P2, P3, P4, P7, and P8 (Table 2). Molecular

imaging techniques used the same acquisition parameters published previously.<sup>22</sup> Briefly, standardized uptake value ratio (SUVR) images were created for each tracer based on specific acquisition time window and reference regions (50–70 min post injection SUVR based on cerebellar grey matter for PIB; 80–100 min post injection based on inferior cerebellar grey matter for flortaucipir). Images were visually interpreted following validated procedures.<sup>23,24</sup>

### Magnetic resonance imaging (MRI)

Structural T1 neuroimaging was performed in all cases via 3T MRI, except for patient 1. As described elsewhere, MRI data were automatically segmented using the New Segment toolbox implemented in the Statistical Parametric Mapping (SPM-12) software (Wellcome Trust Centre for Neuroimaging, Institute of Neurology at University College London).<sup>25</sup> Diffeomorphic Anatomical Registration Through Exponentiated Lie Algebra (DARTEL) was used to generate a study-specific template by aligning the gray matter images nonlinearly to a common space. Native gray and white matter images were spatially normalized to the DARTEL template using individual flow fields (modulation was applied to preserve the total amount of signal). Images were smoothed using an 8 mm full width at half maximum (FWHM) isotropic Gaussian kernel. For each subjects' MRI, we generated a W-map depicting the age-corrected z-score of volume loss.<sup>26</sup> Negative W-scores represent below-average volume.  $<-1.50$  are below seventh percentile compared to healthy controls and are considered clinically abnormal.<sup>26</sup>

### Results

The primary neuropathologic diagnosis in patients P1 through P7 was PSP (Table 1). The collective finding from neurophysiological manifestations in patients P1-P7 was that a primary pathology of 4R tauopathy is associated with an increased spectral density within the alpha (8–12 Hz) oscillatory band (Fig. 1, P1 and P2). However, the change in alpha spectral density was markedly modulated by the degree of AD co-pathology. Specifically, we observed that with increasing AD co-pathology the pattern of spectral change was dominated by reduced alpha power density (Fig. 1, P3-7). For example, P1 and P2 showed the least degree of AD co-pathology (CERAD: A1 B0 C0, and A1 B1 C0, in P1 and P2 respectively), and their spectral signatures showed an increased alpha power density predominantly over the frontal cortices (Fig. 1). In contrast, P6 and P7 showed the greatest degree of AD co-pathology (CERAD: A1 B2 C0 with frequent diffuse plaques, and A3 B2 C2 with frequent diffuse plaqu, in P6 and P7 respectively), and the spectral change was similar

to what is typically observed in patients with AD, showing reduced alpha spectral power over the inferior and posterior temporal, precuneus and posterior parietal-occipital cortices. P3 and P4, who had intermediate AD co-pathology in our cohort showed similar changes of alpha reductions to a lesser degree (Fig. 1).<sup>27,28</sup>

In patients P8, P9, and P10, the primary neuropathologic diagnosis was CBD. P8, P9, and P10 also showed variable degree of AD co-pathology (Table 1). The neurophysiological manifestations in alpha band in primary CBD patients also reflected findings similar to that of PSP, showing increased alpha power density (Fig. 1, P8). The presence of AD co-pathology appeared to modulate the change in alpha spectral power, where alpha power density also showed reductions in patients with moderate neuritic plaques (Fig. 1, P9). It is noteworthy, however, that this overpowering effect of an AD-like alpha signature appeared less prominent in patients with primary CBD neuropathology compared to those with a primary PSP neuropathology. The spectral changes within delta-theta (2–7 Hz) frequency band didn't show noticeable changes in either patient group (Fig. 2).

### Changes in sleep architecture

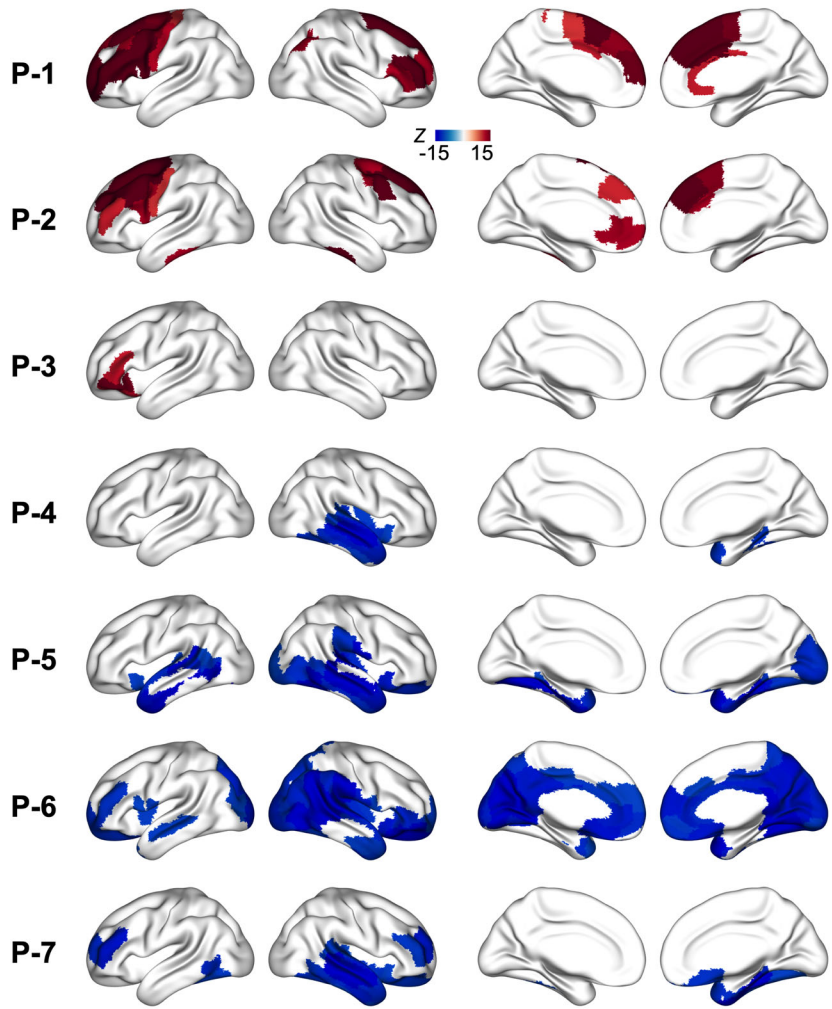
In patients P2, P6, and P7, whose primary neuropathology was PSP, PSG analyses showed decreased sleep efficiency and maintenance, as well as increased REM latency and decreased time in N2/N3 and REM sleep (Table 3). These findings were consistent with sleep reports from a prior PSP series.<sup>3</sup> P7 had more N3 and REM sleep and took less time to fall asleep compared to P2 and P6. With respect to CNS-modifying medications, P6 was on amitriptyline at the time of PSG; P7 was on carbidopa-levodopa and doxepin; and P2 was on buspirone, melatonin, and lorazepam. In addition, P2 had mild sleep apnea. P2 and P6 both were noted to have periodic limb movement disorder. P7 and P2 had possible REM behavior disorder on a caregiver questionnaire, a measure that was not available for P6.

### Structural MRI and molecular imaging findings

For P2 through P10, structural MRI derived volumetric assessment showed patterns of cortical grey matter volume loss when compared to age-matched controls (534 healthy older controls; age range 44–99 years,  $M \pm SD$ :  $68.7 \pm 9.1$ ;  $n = 220$  male;  $n = 302$  female) adjusted for age, sex, total intracranial volume, and magnet strength (Fig. 3). Overall, the atrophy maps reflect the relative heterogeneity of regional patterns of neurodegeneration in 4R-tauopathy syndromes. Six out of 10 patients (P2, P3,



Spectral changes in patients with primary PSP



ADNC

**A0 B1 C0**

Neuritic: *Absent*  
Diffuse: *Absent*

**A1 B1 C0**

Neuritic: *Absent*  
Diffuse: *Sparse*

**A1 B1 C0**

Neuritic: *Absent*  
Diffuse: *Sparse*

**A1 B1 C0**

Neuritic: *Absent*  
Diffuse: *Sparse*

**A1 B2 C0**

Neuritic: *Absent*  
Diffuse: *Sparse*

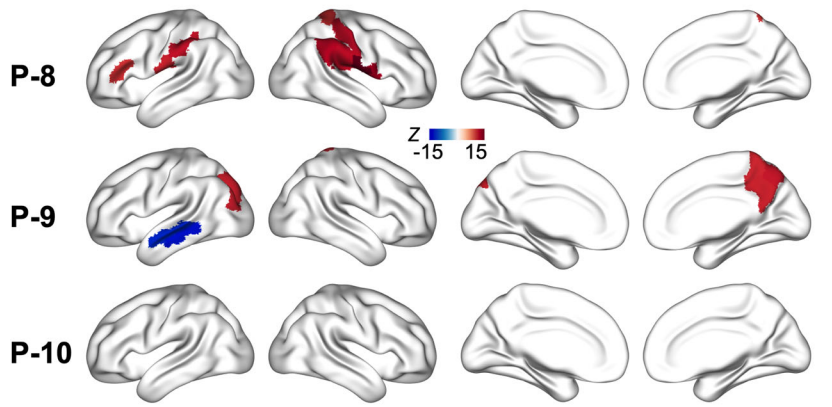
**A1 B2 C0**

Neuritic: *Absent*  
Diffuse: *Frequent*

**A3 B2 C2**

Neuritic: *Moderate*  
Diffuse: *Frequent*

Spectral changes in patients with primary CBD



ADNC

**A1 B1 C1**

Neuritic: *Sparse*  
Diffuse: *Moderate*

**A2 B1 C2**

Neuritic: *Moderate*  
Diffuse: *Frequent*

**A1 B1C2**

Neuritic: *Moderate*  
Diffuse: *Frequent*

**Figure 1.** Spectral signatures in alpha (8–12 Hz) band in patients with 4RT neuropathology. Patients P1 through P7 include patients whose primary neuropathology was PSP, ordered according to the degree of AD copathology in neuropathological assessment, where P1 has the least AD copathology and P7 has the highest AD copathology. Patients P8, P9, and P10 include patients whose primary neuropathology was CBD, ordered according to the degree of AD copathology in neuropathological assessment, where P8 has the least AD copathology and P10 has the highest AD copathology. Each brain rendering depicts the spatial patterns of alpha band spectral power density shown as z-score maps compared to an age matched control cohort ( $n = 40$  healthy elderly; age  $71.38 \pm 8.23$ ; female = 19, male = 21). Z-maps are thresholded to show values  $-10 > z > 10$ . (AD, Alzheimer's disease; ADNC, Alzheimer's disease neuropathologic change; CBD, corticobasal degeneration; PSP, progressive supranuclear palsy).

P5, P7, P8, and P9) were evaluated with amyloid-PET and except one patient (P7) all showed a negative reading, both on visual read and quantification (Centiloid values  $<24.4$ ). Amyloid-PET for P7 was positive (visually, and with a quantification of 69 Centiloids), and was consistent with P7's highest degree of AD neuropathological features (Table 1). Tau PET was performed in five out of ten patients (P2, P3, P4, P7, and P8) and was read as negative (i.e., non-AD tau pattern) for all patients.

## Discussion

This is the first report of a comprehensive spatiotemporal mapping of altered neural oscillations in patients with autopsy-confirmed 4RT. We found an increased alpha signature in patients with 4RT with minimal AD-copathology. Importantly, the presence of AD-copathology modulated this spectral change to the opposite extreme to show a decreased alpha signature, specifically involving the inferolateral temporal and parietal cortices—regions that are highly vulnerable to AD-tau. Previous studies have shown that reduced alpha oscillatory activity in AD is correlated with a greater burden of tau.<sup>9,10</sup> Collectively, the current study demonstrates that impacts from 4R tauopathy is distinct from an AD-tauopathy, while in the presence of comorbidity the overall manifestation is highly sensitive to the changes associated with AD tauopathy.

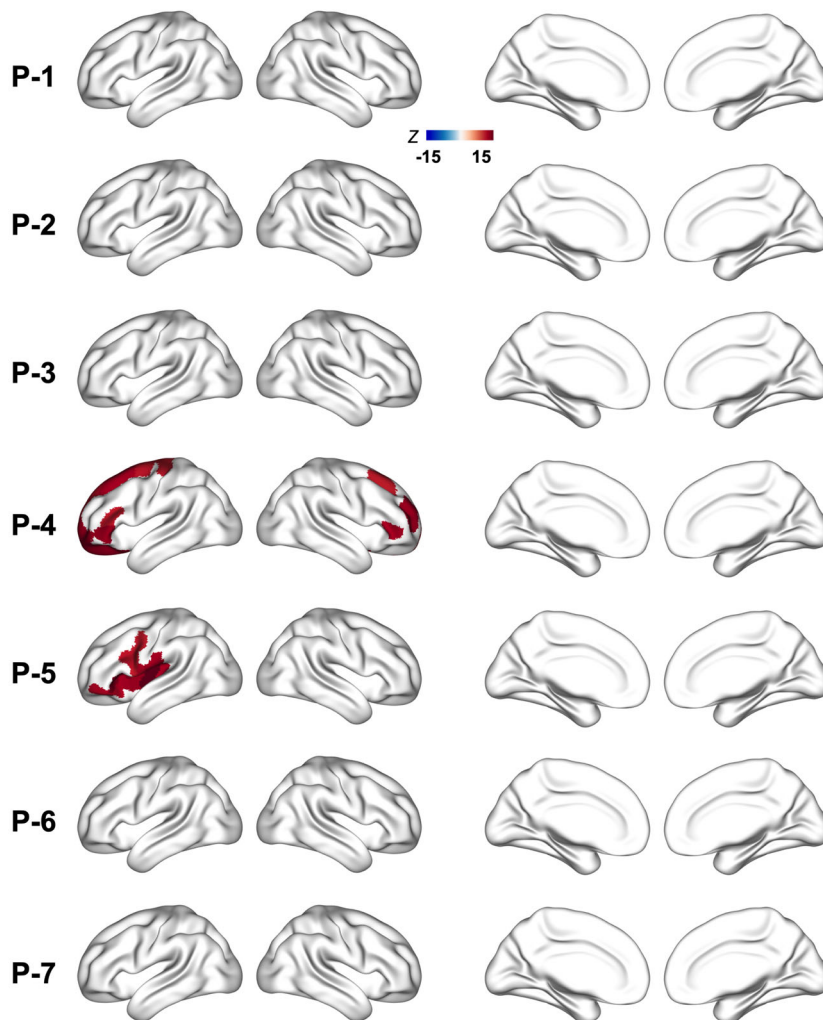
The increased alpha signature in 4RT and the reduced alpha signature in AD, closely map on to their diverging wakefulness phenotypes, implicating selectively vulnerable impacts in the two conditions.<sup>29</sup> The findings from the current study are of particular interest, given the emerging evidence suggesting that disrupted sleep–wake balance is closely associated with abnormally phosphorylated tau.<sup>30,31</sup> An increased alpha signature in PSP is consistent with the poor sleep drive in these patients. While the oscillatory changes observed in primary CBD patients were less robust compared to primary PSP patients neuropathology, this lower degree of alpha increase maybe consistent with the low levels of sleep abnormalities and

prevalence of sleep complaints in CBD compared to PSP<sup>32</sup>. Importantly, the current study demonstrates that AD-copathology is a significant modulator of alpha oscillations in 4RT, and it remains to be determined how AD copathology influence the sleep–wake clinical phenotype in these patients. Among the subset of patients who completed PSG, the patient who had the highest ADNC scores (P7) showed a shorter latency to sleep-onset and higher N3 and REM duration than those with low ADNC. While the current series is limited in its conclusions at group level, this observation indeed suggests possible modulatory effects of sleep–wake phenotype in comorbid PSP-AD. It is important to determine in future studies how altered spectral signatures in the presence of comorbid AD are translated across different brain states from awake-resting to sleep.

Previously we reported that subcortical wake-promoting neurons degenerate at the earliest stages of AD when abnormal tau accumulates in the brainstem regions of ascending reticular activating system during Braak NFT stage 0, even before the appearance of A $\beta$  plaques.<sup>5,6</sup> The current results demonstrate that reduced alpha oscillatory activity, the signature spectral change in AD, is prominent in patients with primary PSP neuropathology who harbor intermediate-to-low degree of AD pathology. This is consistent with the notion that AD associated changes occur at the earliest stage of AD neuropathological spectrum. In the current case series, we do not have a sensitive, quantitative measure to index the earliest AD-tau accumulation. Hence, it is not feasible to tease apart whether the neurophysiological abnormalities observed with increasing AD copathology is driven by tau or by amyloid. Notwithstanding this ambiguity, the degree of amyloid pathology in the current series of patients with primary PSP pathology was small, ranging from low to intermediate ADNC, indicating that observed changes may be consequential to early AD-tauopathy or to an additive effect of both tau and amyloid. It is important to determine in future studies how these distinct effects on wake-promoting and sleep-promoting neurons in AD and PSP tauopathies translates into clinical measures of wakefulness.



Delta-theta (2-7 Hz) spectral changes in patients with primary PSP



Delta-theta (2-7 Hz) spectral changes in patients with primary CBD

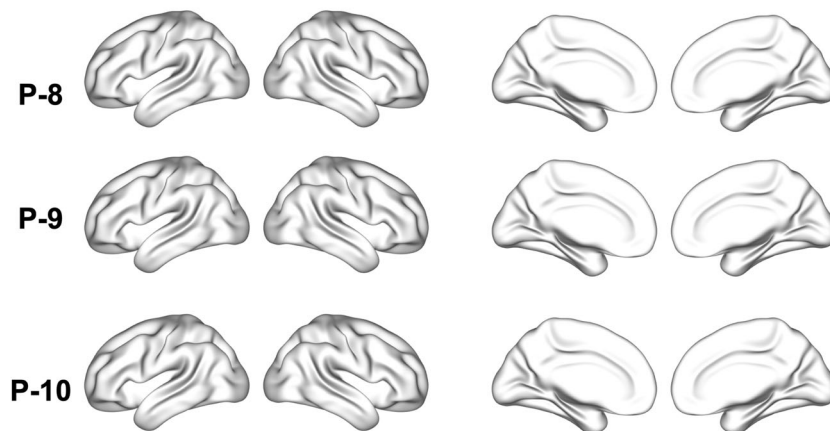


**Figure 2.** Spectral signatures in delta-theta (2–7 Hz) band in patients with 4RT neuropathology. Patients P1 through P7 include patients whose primary neuropathology was PSP and ordered according to the degree of AD copathology in neuropathological assessment, where P1 has the least AD copathology and P7 has the highest AD copathology. Patients P8, P9, and P10 include patients whose primary neuropathology was CBD and ordered according to the degree of AD copathology in neuropathological assessment where P8 has the least AD copathology and P10 has the highest AD copathology. Each brain rendering depicts the spatial patterns of delta-theta band spectral power density shown as z-score maps compared to an age matched control cohort ( $n = 40$  healthy elderly; age  $71.38 \pm 8.23$ ; female = 19, male = 21). Z-maps are thresholded to show values  $-10 > z > 10$  (: AD, Alzheimer's disease; CBD, corticobasal degeneration; PSP, progressive supranuclear palsy).

**Table 3.** Polysomnographic features.

Patient	Sleep efficiency (%)	Sleep onset latency (min)	Wake time after sleep onset (min)	REM/N2/N3 percent duration of total sleep time	Latency to REM (min)	Apnea-hypopnea index (AHI)	Periodic limb movement index (PLMI)	Total sleep time (min)
P2	54.8	44.5	205	15.0/51.4/14.7	201.0	11.7	79.1	303
P6	59.5	52.0	151.0	18.0/48.1/14.9	18.0	0.8	25.8	303.0
P7	44.7	10.5	263	25.7/25.3/31.3	53.0	0	12.5	226

Our study is not without limitations. Although the distinct patterns associated with these tauopathies are consistent with the known divergent wakefulness patterns of AD and 4RT clinical syndromes, the small sample size limited our ability to perform group level correlations with specific clinical indices of wakefulness phenotypes. Such an analysis mandates a larger clinical cohort to derive meaningful inferences given the clinical heterogeneity inherent to 4RT syndromes. It is also important in future studies to further examine how spatial patterns of spectral signatures are changed in 4RT with increasing AD-copathology, at group level. Nonetheless, the current study is an important steppingstone in the design and implementation of larger cohort studies including diverse demographics in the future to investigate the associations between spectral changes and behavioral measures of wakefulness.

In summary, the current case series suggest that neurophysiological manifestations are important indices of distinct neurodegenerative processes and further investigation into the underlying cellular and molecular origins of neurophysiologic changes may help distinguish specific effects of different pathological tau variants.

## Acknowledgments

We would like to thank all the study participants and their families for their generous support to our research. We would also like to acknowledge Avid Radiopharmaceuticals for enabling the use of the 18F-flortaucipir tracer by providing the precursor.

## Author Contributions

KGR, SSN, conceptualized and designed the study, interpreted the results, and contributed to manuscript writing. KGR, HEK and NS contributed to electrophysiological readings, NS and HL performed data analyses and contributed to manuscript writing. LY, CMW, TN, and LTG contributed to sleep data collection, analyses and interpretation; KK contributed to analysis of time series data; CY, RLJ and GDR contributed to PET data collection and interpretations; MLG contributed to some clinical data collection; SP, WWS and LTG contributed to clinical data collection and neuropathological assessments and interpretations; BLM, GDR, LTG, and KPR contributed to clinical evaluations, diagnostic interpretations and to study conceptualization.

## Conflict of interest

The authors of this manuscript have no competing interests relevant to the content presented in the manuscript.

## Data availability statement

All data associated with this study are present in the paper or in Data S1. Anonymized subject data will be shared on request from qualified investigators for the purposes of replicating procedures and results, and for other noncommercial research purposes within the limits of participants' consent. Correspondence and material requests should be addressed to kamalini.ranasinghe@ucsf.edu.

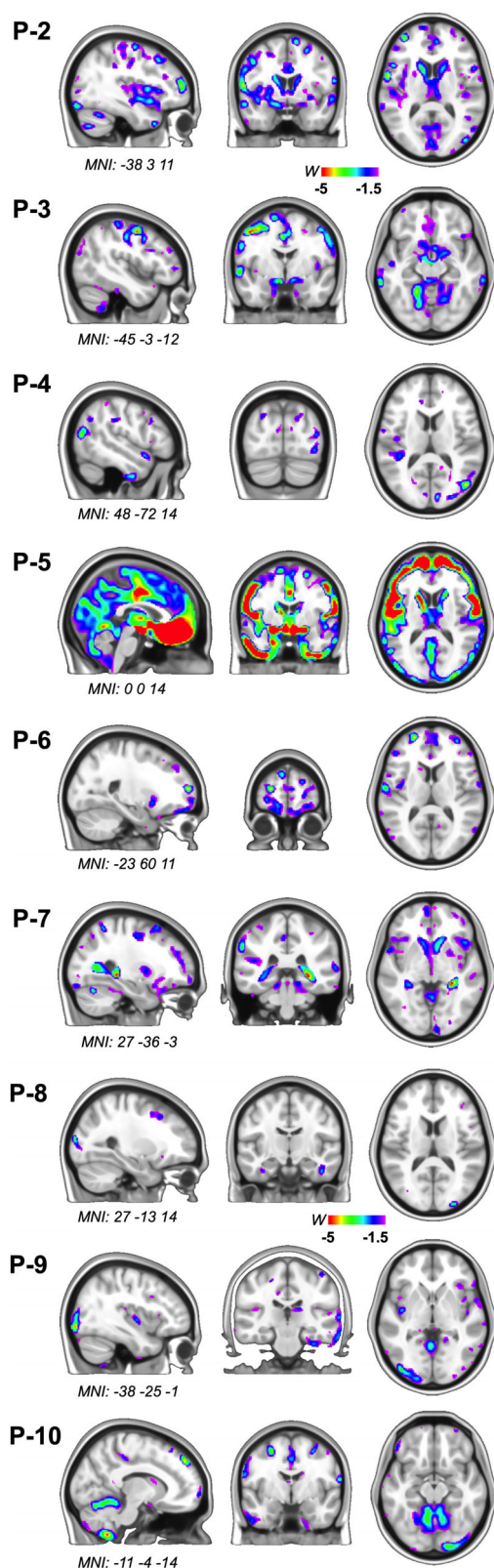


**Figure 3.** Cortical grey matter volume loss in patients with 4RT neuropathology. Color maps indicate grey matter atrophy as a W-map gradient going from blue to green to red are shown for the P2 through P10 cases (P1 is excluded from this analysis as there was no MRI scan available that fulfilled the research acquisition criteria for volumetric assessment). P2-P7 indicate patients with primary PSP neuropathology and P8-P10 indicate patients with primary CBD neuropathology. The MNI coordinates represent the sagittal, coronal, and axial slices for each patient capturing a representative visualization of grey matter atrophy. Negative W-scores represent below-average volume, and blue represents a W-score (analogous to z-score) of  $-1.5$ , while red represents a score of  $-5$ . W-maps are generated based on a healthy control group from the normative databases at our center ( $n = 534$  healthy elderly; age:  $68.7 \pm 9.1$ ; female = 302, male = 220 male). MRI imaging that could be directly compared to this established control group was not available for P1 (CBD, corticobasal degeneration; MNI, Montreal Neurological Institute; PSP, progressive supranuclear palsy).

## REFERENCES

- Rösler TW, Tayanian Marvian A, Brendel M, et al. Four-repeat tauopathies. *Prog Neurobiol.* 2019;180:101644.
- Aldrich MS, Foster NL, White RF, Bluemlein L, Prokopowicz G. Sleep abnormalities in progressive supranuclear palsy. *Ann Neurol.* 1989;25:577-581.
- Walsh CM, Ruoff L, Walker K, et al. Sleepless night and day, the plight of progressive supranuclear palsy. *Sleep.* 2017;40:zsx154.
- Hokelekli FO, Ali F, Carlos AF, et al. Sleep disturbances in the speech-language variant of progressive supranuclear palsy. *Parkinsonism Relat Disord.* 2021;91:9-12.
- Lew CH, Petersen C, Neylan TC, Grinberg LT. Tau-driven degeneration of sleep- and wake-regulating neurons in Alzheimer's disease. *Sleep Med Rev.* 2021;60:101541.
- Oh JY, Walsh CM, Ranasinghe K, et al. Subcortical neuronal correlates of sleep in neurodegenerative diseases. *JAMA Neurol.* 2022;79:498-508.
- Gibbons GS, Kim SJ, Robinson JL, et al. Detection of Alzheimer's disease (AD) specific tau pathology with conformation-selective anti-tau monoclonal antibody in co-morbid frontotemporal lobar degeneration-tau (FTLD-tau). *Acta Neuropathol Commun.* 2019;7:34.
- Chang BS, Schomer DL, Niedermeyer E. Normal EEG and sleep: adults and elderly. In: Schomer DL, Lopes da Silva F, eds. *Niedermeyer's Electroencephalography: Basic Principles, Clinical Applications and Related Fields.* 6th ed. Lippincott Williams & Wilkins; 2011:183-215.
- Ranasinghe KG, Cha J, Iaccarino L, et al. Neurophysiological signatures in Alzheimer's disease are distinctly associated with TAU, amyloid-beta

- accumulation, and cognitive decline. *Sci Transl Med.* 2020;12:eaaz4069.
10. Ranasinghe KG, Petersen C, Kudo K, et al. Reduced synchrony in alpha oscillations during life predicts post mortem neurofibrillary tangle density in early-onset and atypical Alzheimer's disease. *Alzheimers Dement.* 2021;17:2009-2019.
  11. Spina S, Brown JA, Deng J, et al. Neuropathological correlates of structural and functional imaging biomarkers in 4-repeat tauopathies. *Brain.* 2019;142:2068-2081.
  12. Montine TJ, Phelps CH, Beach TG, et al. National Institute on Aging-Alzheimer's Association guidelines for the neuropathologic assessment of Alzheimer's disease: a practical approach. *Acta Neuropathol.* 2012;123:1-11.
  13. McKhann GM, Albert MS, Grossman M, Miller B, Dickson D, Trojanowski JQ. Clinical and pathological diagnosis of frontotemporal dementia: report of the Work Group on Frontotemporal Dementia and Pick's Disease. *Arch Neurol.* 2001;58:1803-1809.
  14. Mackenzie IR, Neumann M, Bigio EH, et al. Nomenclature for neuropathologic subtypes of frontotemporal lobar degeneration: consensus recommendations. *Acta Neuropathol.* 2009;117:15-18.
  15. Attems J, Toledo JB, Walker L, et al. Neuropathological consensus criteria for the evaluation of Lewy pathology in post-mortem brains: a multi-centre study. *Acta Neuropathol.* 2021;141:159-172.
  16. Roemer SF, Grinberg LT, Crary JF, et al. Rainwater Charitable Foundation criteria for the neuropathologic diagnosis of progressive supranuclear palsy. *Acta Neuropathologica.* 2022;144:603-614.
  17. Mirra SS, Heyman A, McKeel D, et al. The Consortium to Establish a Registry for Alzheimer's Disease (CERAD). Part II. Standardization of the neuropathologic assessment of Alzheimer's disease. *Neurology.* 1991;41:479-486.
  18. Oostenveld R, Fries P, Maris E, Schoffelen JM. FieldTrip: open source software for advanced analysis of MEG, EEG, and invasive electrophysiological data. *Comput Intell Neurosci.* 2011;2011:156869.
  19. Nolte G. The magnetic lead field theorem in the quasi-static approximation and its use for magnetoencephalography forward calculation in realistic volume conductors. *Phys Med Biol.* 2003;48:3637-3652.
  20. Fan L, Li H, Zhuo J, et al. The human brainnetome atlas: a new brain atlas based on connectonal architecture. *Cereb Cortex.* 2016;26:3508-3526.
  21. Xia M, Wang J, He Y. BrainNet Viewer: a network visualization tool for human brain connectomics. *PLoS One.* 2013;8:e68910.
  22. La Joie R, Visani AV, Lesman-Segev OH, et al. Association of APOE4 and clinical variability in Alzheimer disease with the pattern of tau- and amyloid-PET. *Neurology.* 2021;96:e650-e661.
  23. Lesman-Segev OH, La Joie R, Iaccarino L, et al. Diagnostic accuracy of amyloid versus (18) F-fluorodeoxyglucose positron emission tomography in autopsy-confirmed dementia. *Ann Neurol.* 2021;89:389-401.
  24. Fleisher AS, Pontecorvo MJ, Devous MD Sr, et al. Positron emission tomography imaging with [18F] flortaucipir and postmortem assessment of Alzheimer disease neuropathologic changes. *JAMA Neurol.* 2020;77:829-839.
  25. Kim EJ, Brown JA, Deng J, et al. Mixed TDP-43 proteinopathy and tauopathy in frontotemporal lobar degeneration: nine case series. *J Neurol.* 2018;265:2960-2971.
  26. Ossenkoppele R, Cohn-Sheehy BI, La Joie R, et al. Atrophy patterns in early clinical stages across distinct phenotypes of Alzheimer's disease. *Hum Brain Mapp.* 2015;36:4421-4437.
  27. Ranasinghe KG, Cha J, Iaccarino L, et al. Neurophysiological signatures in Alzheimer's disease are distinctly associated with TAU, amyloid- $\beta$  accumulation, and cognitive decline. *Sci Transl Med.* 2020;12:eaaz4069.
  28. Ranasinghe KG, Verma P, Cai C, et al. Altered excitatory and inhibitory neuronal subpopulation parameters are distinctly associated with tau and amyloid in Alzheimer's disease. *eLife.* 2022;11:e77850.
  29. Oh J, Eser RA, Ehrenberg AJ, et al. Profound degeneration of wake-promoting neurons in Alzheimer's disease. *Alzheimers Dement.* 2019;15:1253-1263.
  30. Holth J, Patel T, Holtzman DM. Sleep in Alzheimer's disease – beyond amyloid. *Neurobiol Sleep Circadian Rhythms.* 2017;2:4-14.
  31. Holth JK, Mahan TE, Robinson GO, Rocha A, Holtzman DM. Altered sleep and EEG power in the P301S Tau transgenic mouse model. *Ann Clin Transl Neurol.* 2017;4:180-190.
  32. Abbott SM, Videnovic A. Sleep disorders in atypical parkinsonism. *Mov Disord Clin Pract.* 2014;1:89-96.

## Supporting Information

Additional supporting information may be found online in the Supporting Information section at the end of the article.

**Data S1.** Clinical history and neurological examination findings of each case.

**Table S1.** Neuropsychological test performance.